

Journal Pre-proof

Swelling as a promoter of migration of plastic additives in the interaction of fatty food simulants with polylactic acid- and polypropylene-based plastics

Csaba Kirckeszner, Noémi Petrovics, Tamás Tábi, Norbert Magyar, József Kovács, Bálint Sámuel Szabó, Zoltán Nyiri, Zsuzsanna Eke



PII: S0956-7135(21)00492-8

DOI: <https://doi.org/10.1016/j.foodcont.2021.108354>

Reference: JFCO 108354

To appear in: *Food Control*

Received Date: 9 March 2021

Revised Date: 15 June 2021

Accepted Date: 16 June 2021

Please cite this article as: Kirckeszner C., Petrovics N., Tábi T., Magyar N., Kovács J., Szabó B.S., Nyiri Z. & Eke Z., Swelling as a promoter of migration of plastic additives in the interaction of fatty food simulants with polylactic acid- and polypropylene-based plastics, *Food Control*, <https://doi.org/10.1016/j.foodcont.2021.108354>.

This is a PDF file of an article that has undergone enhancements after acceptance, such as the addition of a cover page and metadata, and formatting for readability, but it is not yet the definitive version of record. This version will undergo additional copyediting, typesetting and review before it is published in its final form, but we are providing this version to give early visibility of the article. Please note that, during the production process, errors may be discovered which could affect the content, and all legal disclaimers that apply to the journal pertain.

© 2021 The Author(s). Published by Elsevier Ltd.

CRedit (Contributor Roles Taxonomy) authorship contribution statement

Csaba Kirckeszner: conceptualization, design and conduct the experiments, data evaluation and visualization, formal analysis, writing – original draft

Noémi Petrovics: conceptualization, design and conduct the experiments, data evaluation and visualization, formal analysis, writing – original draft

Tamás Tábi: production and analysis of plastics, data interpretation, writing – review & editing, funding acquisition

Norbert Magyar: data visualization, formal analysis, writing – review & editing

József Kovács: data visualization, formal analysis, writing – review & editing, funding acquisition

Bálint Sámuel Szabó: writing – review & editing, conceptualization

Zoltán Nyiri: writing – review & editing, conceptualization

Zsuzsanna Eke: conceptualization, supervision, writing – review & editing, funding acquisition

1 **Swelling as a promoter of migration of plastic additives in the interaction of**
2 **fatty food simulants with polylactic acid- and polypropylene-based plastics**

3
4 Csaba Kirchkeszner^{a,b,‡}, Noémi Petrovics^{a,b,‡}, Tamás Tábi^{c,d}, Norbert Magyar^e, József
5 Kovács^f, Bálint Sámuel Szabó^{a,b}, Zoltán Nyiri^b, Zsuzsanna Eke^{a,g*}

6
7 ^a Hevesy György PhD School of Chemistry, Eötvös Loránd University, Pázmány Péter stny.
8 1/A, H-1117 Budapest, Hungary

9 ^b Joint Research and Training Laboratory on Separation Techniques, Institute of Chemistry,
10 Eötvös Loránd University, Pázmány Péter stny. 1/A, H-1117 Budapest, Hungary

11 ^c Department of Polymer Engineering, Faculty of Mechanical Engineering, Budapest
12 University of Technology and Economics, Műegyetem rkp. 3, H-1111 Budapest, Hungary

13 ^d MTA-BME Research Group for Composite Science and Technology, Műegyetem rkp. 3, H-
14 1111 Budapest, Hungary

15 ^e Department of Methodology for Business Analyses, Faculty of Commerce, Hospitality and
16 Tourism, Budapest Business School, Alkotmány u. 9–11, H-1054 Budapest, Hungary

17 ^f Department of Geology, Institute of Geography and Earth Sciences, Eötvös Loránd
18 University, Pázmány Péter stny. 1/C, H-1117 Budapest, Hungary

19 ^g Wessling International Research and Educational Center, Anonymus u. 6, H-1045 Budapest,
20 Hungary

21
22 * Corresponding author. E-mail address: zsuzsanna.eke@ttk.elte.hu (Zsuzsanna Eke)
23 Phone number: +36-30-598-0300

24 [‡] These two authors contributed equally to the work.

25 E-mail addresses: csaba.kirchkeszner@ekol.chem.elte.hu,
26 noemi.petrovics@ekol.chem.elte.hu, tabi@pt.bme.hu, magyar.norbert@uni-bge.hu,
27 kevesolt@geology.elte.hu, balint.szabo@ekol.chem.elte.hu, zoltan.nyiri@ekol.chem.elte.hu

28 **Abstract**

29 The migration of various plastic additives (antioxidants: BHT, Ionox 220, Irgafos 168;
30 UV absorber: Uvinul 3039; plasticizers: TBAC and TOTM) from polypropylene and
31 polylactic acid was investigated in a series of experiments conducted over a period of 13 days.
32 As fatty food simulants, both ethanol 95 v/v% and isooctane were used. Non-Fickian
33 behaviour was observed on multiple occasions. The kinetic curves of both migration
34 concentrations and swelling were evaluated using variography to determine objectively the
35 starting points of long-lasting plateaus as well as short halts in the increase. A strong
36 correlation between migration and swelling was observed: the kinetic curves showed that
37 migration always followed swelling. Also, more intensive swelling results in the increased
38 migration of the additives. Consequently, migration testing can be improved by considering
39 the swelling of the plastic.

40

41 **Keywords**

42 polylactic acid (PLA), polypropylene (PP), food contact materials (FCM), migration kinetics,
43 swelling effect, variography

44

45 **Highlights**

- 46 • Migration and swelling kinetics of polylactic acid and polypropylene were studied.
- 47 • Swelling strongly affects plastic additive migration from food contact materials.
- 48 • The effect of molecular weight on additive migration can be overruled by plasticizers.
- 49 • Variography was successfully applied to identify steady-states on kinetic curves.

50 1. Introduction

51 Plastic food contact materials (FCPs) play an indispensable role in food production,
52 storage, transport and safety. Nowadays, the most commonly used FCPs are petrochemical-
53 based polymers, such as polyethylene (PE) and polypropylene (PP). Its low price, good
54 malleability, and strong water barrier properties make PP a remarkable raw material in the
55 manufacture of food packaging. However, the rapid growth of environmental awareness has
56 increased demand for the use of biodegradable polymers. For food industry applications, the
57 most prominent biopolymer is polylactic acid (PLA), due to its high mechanical strength,
58 good optical properties, low toxicity, and relatively low price.

59 Along with polymers, FCPs also contain additives; antioxidants, UV stabilizers, slip
60 agents, nucleating agents, plasticizers and various other additives are used to prevent the
61 degradation of plastic products and improve the processability of the raw material. These
62 chemical compounds and their contaminants or degradation products can migrate from the
63 FCP into the food, which might pose a serious risk to human health. Migration studies are
64 therefore required in the case of plastic materials that are to be used as food contact materials.
65 Commission Regulation (EU) 10/2011 of 14 January 2011 on “Plastic materials and articles
66 intended to come into contact with food” (**Commission Regulation (EU) 10/2011, 2011**) lays
67 down rules for the basic circumstances (e.g. contact time, temperature) of such tests. Some
68 standard test settings are also determined, e.g. long-term storage at room temperature or
69 below are to be modelled using a 10 day migration test at elevated temperatures (40 °C or 60
70 °C).

71 Furthermore, the use of six food simulants instead of real food is prescribed. The
72 choice of appropriate simulant depends on the characteristics of the food intended to come
73 into contact with the FCP. For instance, vegetable oil with less than 1% unsaponifiable matter
74 is specified as a substitute for lipophilic food (**Commission Regulation (EU) 10/2011, 2011**).
75 Nevertheless, this food simulant is rarely used in specific migration studies, since it is not
76 compatible with either gas (GC) or reversed-phase high-performance liquid chromatographic
77 (RP-HPLC) analytical systems. Usually, 2,2,4-trimethylpentane (isooctane) and ethanol 95
78 v/v% are used instead (**Aznar et al., 2019; Garde et al., 2001; Lu et al., 2021; Ramos et al.,**
79 **2014; Vera et al., 2018; Yang et al., 2016**). These are the solvents also specified in the
80 current consolidated version of the aforementioned regulation (**Commission Regulation**
81 **(EU) 10/2011, 2011**) for cases when it is not technically feasible to work with vegetable oil.
82 For such cases, however, the use of both solvents is required. With this approach, the

83 analytical work becomes incomparably easier, even though it duplicates the number of
84 samples to be analyzed. In the end, to ensure consumer safety, any decision on compliance of
85 the FCP tested must be based on the highest observed concentrations. This means the number
86 of samples to be analyzed can be kept under control if the solvent providing a more intensive
87 migration is known prior to the testing.

88 Migration is a complex process, the result of diffusion, dissolution, and equilibrium
89 (Manzanarez-López et al., 2011; Samsudin et al., 2018). Therefore, a deeper understanding
90 of this phenomenon is based on kinetic tests, in which the time dependence of mass transfer is
91 investigated. Several kinetic studies on the migration of various compounds into food
92 simulants are available. These studies usually aim at demonstrating the applicability of the
93 tested compounds to become the active agent of active packaging and thus focus on the
94 release of antioxidants (Chang et al., 2019; Garde et al., 2001; Jamshidian et al., 2012,
95 2013; Kang et al., 2018; Manzanarez-López et al., 2011; Ramos et al., 2014) or
96 antimicrobial compounds (Kuorwel et al., 2013; Mascheroni et al., 2010) from thin plastic
97 films (typically 50–200 μm). Recently, Kang et al. (2018) investigated concentrations of
98 BHT and Irganox 1010 in food simulants migrating from PP after pre-treatments mimicking
99 severe food processing conditions, such as sterilization at 121 °C, microwave cooking, and
100 deep freezing. The concentrations observed were presented as a function of contact time, thus
101 demonstrating how the conditions under consideration can amplify migration. A more
102 widespread approach is to assume that Fick's second law of diffusion applies and calculate
103 diffusion coefficients by determining the correlation between migrated concentrations (M_t)
104 normalized with migrated concentration at equilibrium (M_∞) and contact time (t) (Chang et
105 al., 2019; Garde et al., 2001; Gavriil et al., 2018; Jamshidian et al., 2012, 2013; Kuorwel
106 et al., 2013; Manzanarez-López et al., 2011; Mascheroni et al., 2010; Ramos et al., 2014).

107 However, non-Fickian behaviour has been reported on multiple occasions. In a study
108 on the release of α -tocopherol from PLA films (α -tocopherol content: 2.58 w%) to oil and
109 ethanol, Manzanarez-López et al. (2011) observed an apparent equilibrium at 73 hours in
110 ethanol at 33 °C. After 106 hours of contact, the concentration of α -tocopherol in the ethanol
111 phase started to increase again, reaching a new equilibrium at 269 hours. Apparent
112 equilibrium was also found by Iñiguez-Franco et al. (2012), in the case of catechin and
113 epicatechin migration from PLA (at contact temperatures of 20 °C and 30 °C). Feigenbaum
114 et al. (2000) reported that the diffusion coefficient of aromatic antioxidants migrating from
115 PP random copolymer into isooctane increased constantly before the concentration of the
116 antioxidants in the isooctane phase reached a plateau. Garde et al. (2001) pointed out that the

117 penetration of *n*-heptane into PP must cause a time dependence in the diffusion coefficient of
118 antioxidants released from the polymer until the mass transfer of the *n*-heptane is completed.
119 The Fickian migration curves observed were explained as being caused by the swelling
120 process being fast compared to the migration of antioxidants. After the swelling process was
121 completed, the diffusion coefficient became constant, and this was the value measured
122 experimentally. **Mascheroni et al. (2010)** applied Fickian models with three different
123 boundary conditions to the prediction of the diffusivity of propolis compounds from PLA
124 films to ethanol and water. The failure of these theoretical models to predict the migration
125 process was attributed to the swelling effect of ethanol.

126 **Bodai et al. (2015)** introduced variography into chemometrics. It was used in the
127 evaluation of kinetic curves of the migration of Tinuvin P and Irganox 3114 from high-
128 density polyethylene. In the field of earth and environmental sciences this method has been
129 successfully applied to obtain the necessary sampling frequency in time (**Hatvani et al.,**
130 **2012; Kovács et al., 2012**) and space (**Hatvani et al., 2018; Hatvani et al., 2014, 2017,**
131 **2020; Kern et al., 2020; Trásy et al., 2018**), in other words, to find the distance –be it in
132 space or time – at which the data are auto-uncorrelated. **Bodai et al. (2015)** demonstrated that
133 the original geostatistical method can be used to determine the time necessary to reach a
134 steady-state in the concentration of plastic additives in food simulants. This indicates the
135 likelihood of its applicability to the assessment of migration curves showing non-Fickian
136 behaviour.

137 The plasticizing effect of swelling and its effect of promoting on the migration of
138 polymer additives is widely known. It is usual to explain the relatively high diffusion
139 coefficients obtained using food simulants mimicking fatty food by the swelling of the
140 polymer (**Feigenbaum et al., 2000; Nasiri et al., 2016**). **Samsudin et al. (2014)** observed a
141 large release of astaxanthin from PLA to 95% ethanol and attributed it to disruptions of the
142 microstructure of the PLA film caused by ethanol. In this study, however, the degree of
143 swelling observed in PLA samples was not determined. Greater emphasis was assigned to the
144 swelling of PLA by ethanol by **Iñiguez-Franco et al. (2017)** in their work on the dependence
145 of ethanol sorption by PLA and PLA nanocomposite on ethanol fraction, demonstrating that
146 PLA became more elastic when it was immersed in a solution with a higher ethanol content.
147 Also, the migration of a nanoclay-related surfactant was followed in a 180 day long release
148 study. A connection between the elevated migration rate of surfactant and polymer swelling
149 was assumed in the early stage of release; the time dependence of solvent uptake was not,
150 however, followed. In general, increased migration is often associated with swelling (**Garde**

151 **et al., 2001; Jamshidian et al., 2012; Manzanarez-López et al., 2011; Ramos et al., 2014)**,
152 the latter is, however, rarely measured, even though swelling renders the assumption of
153 Fickian diffusion invalid.

154 In this study, the aim was to take a deeper look at the connection between swelling and
155 migration by correlating their kinetic curves using PLA and PP polymers. Both polymers have
156 well-established uses as FCPs, while their physical-chemical properties differ to a remarkable
157 degree. The experiments conducted in the course of this study were designed bearing the
158 compliance testing of FCPs in mind. A timeframe close to 10 days was adhered to, as this is
159 the maximum necessary testing time according to Commission Regulation (EU) 10/2011
160 **(Commission Regulation (EU) 10/2011, 2011)**. Beside antioxidants (BHT, Ionox 220,
161 Irgafos 168), a UV absorber (Uvinul 3039) and two plasticizers (TBAC, TOTM) were
162 included. These additives not only cover various functionalities, but also differ in molecular
163 weight. To avoid the need for assuming Fickian behaviour the determination of diffusion
164 coefficients was not pursued, and a decision was made to use variography to determine the
165 onset of steady-states.

166 **2. Materials and Methods**

167 **2.1. Chemicals and Materials**

168 IngeoTM Biopolymer 2500HP polylactic acid polymer resin (*D*-lactide content of 0.5
169 *w*%) was purchased from NatureWorks LLC (Minnetonka, Minnesota, USA). Tipplen H145F
170 polypropylene homopolymer resin was bought from MOL Group (Budapest, Hungary). Both
171 polymer types are suitable for the production of food contact materials.

172 The polymers were compounded with five different plastic additives. These were BHT
173 (2,6-di-*tert*-butyl-4-methylphenol, CAS: 128-37-0), Ionox 220 (4,4'-methylene-*bis*(2,6-di-*tert*-
174 *tert*-butylphenol), CAS: 118-82-1), Uvinul 3039 (2-ethylhexyl 2-cyano-3,3-diphenylacrylate,
175 CAS: 6197-30-4), TBAC (tributyl acetyl citrate, CAS: 77-90-7) and TOTM (*tris*(2-
176 ethylhexyl) trimellitate), CAS: 3319-31-1). Besides, the PP resin originally contained the
177 antioxidant Irgafos 168 (*tris*(2,4-di-*tert*-butylphenyl) phosphite, CAS: 31570-04-4) at a
178 concentration of 0.5 *w*%. During sample preparation, mirex (perchloropentacyclodecane,
179 CAS: 2385-85-5) was used as an evaporation standard. BHT, TBAC, TOTM, and mirex were
180 purchased from Sigma-Aldrich Co. (Budapest, Hungary). Ionox 220 was bought from Alfa
181 Aesar (Molar Chemicals, Budapest, Hungary) and the Uvinul 3039 was donated by BASF
182 Hungary Ltd. (Budapest, Hungary).

183 In the migration tests, isooctane (2,2,4-trimethylpentane, CAS: 54-84-1) and ethanol
184 95 v/v% (CAS: 64-17-5) were applied as food simulants of fatty food. HPLC grade isooctane
185 and ethanol were purchased from Thomasker Finechemicals Ltd. (Budapest, Hungary).

186 The concentration of individual stock solutions of plastic additives and that of mirex
187 were 1000 mg/L and 200 mg/L, respectively. A working solution containing all five additives
188 at 150 mg/L was prepared. Calibration solutions for quantitative analysis were diluted to 10
189 different concentration levels from the working solution in the 25 µg/L–100 mg/L range. Each
190 solution contained mirex in a concentration of 10 mg/L. Calibration solutions were prepared
191 in both isooctane and ethanol 95 v/v%. Two linear curves were fitted in each calibration range
192 of target compounds to achieve the appropriate linearity ($R^2 > 0.9900$). The lower and upper
193 concentration levels of the calibration linear curves were defined as the lower and upper limits
194 of quantitation (*LLOQ* and *ULOQ*). At these points, recoveries were calculated. *LLOQ* data
195 are listed in **Table 1**. More detailed information on the calibration curves and representative
196 chromatograms can be found in *Supp. Inf. Table 1*.

197 **2.2. Production of Plastic Samples**

198 Plastic specimens were produced in a three-stage technological process. First, the
199 polymer resins were compounded with the additives using a twin-screw extruder. The
200 resulting filaments were then shredded and repelletized. Eventually, square-shaped sheet
201 specimens were made using injection molding.

202 In the case of PLA, overnight heating at 85 °C was necessary to prevent the hydrolysis
203 of polymer chains during production. In order to avoid possible interference between target
204 compounds and degradation products in quantitative analysis, each polymer was compounded
205 with only one additive. Therefore, the production process resulted in six different types of
206 plastics for both PLA and PP. Additive concentrations were set according to the
207 recommendation of the manufacturers: plastic specimens contained 1.0 w% BHT or Ionox
208 220, 0.75 w% Uvinul 3039, or 5.0 w% TBAC or TOTM. A production blank (i.e. reference
209 sample) was produced, as well.

210 Compounding was performed with LTE 26-44 twin-screw extruder (Labtech
211 Engineering Co., Ltd., Samutprakarn, Thailand) which was equipped with 26 mm diameter
212 screws. Its rotational speed was 50 rpm during processing. The temperature profile of the
213 screw segments was 170–175–180–185–190 °C toward the nozzle. The average output was
214 60 m/min of 3 mm diameter plastic filament. 3 mm long pellets were shredded using a LZ-
215 120/VS pelletizer (Labtech Engineering Co., Ltd., Samutprakarn, Thailand).

216 The injection molding instrument was an Arburg Allrounder Advance 270S 400-170
 217 (Arburg GmbH, Lossburg, Germany) with a 30 mm diameter screw. The temperature profile
 218 increased from 190 °C to 210 °C (PLA) and 170 °C to 190 °C (PP) in 5 °C steps. Molding
 219 temperature was 25 °C. Injection speed was 50 cm³/s. Holding pressure was 500 bar for 20 s
 220 in the case of PLA and 350 bar for 5 s for PP. The residual cooling times of PLA and PP were
 221 40 s and 20 s, respectively. The result of each injection molding cycle was a pair of
 222 80×80×2 mm (height×width×thickness) plastic sheets.

223 **2.3. Characterization of Plastic Materials**

224 For the mechanical and thermal characterization of plastics, differential scanning
 225 calorimetric (DSC) analysis and melt flow rate (*MFR*) measurement were performed. The
 226 DSC thermal analyzer (Q2000) was the product of TA Instruments (New Castle, Delaware,
 227 USA). The DSC curves were recorded in heat/cool/heat scan cycles. The purge gas was
 228 nitrogen. The mass of samples was between 3–6 mg. In the case of PLA, the examined
 229 temperature range was 0–200 °C at 5 °C/min heating and cooling rates. For PP analysis, the
 230 temperature range was –50–200 °C at 10 °C/min heating and cooling rates. The thermograms
 231 were evaluated using TA Universal Analysis Software (TA Instruments, New Castle,
 232 Delaware, USA). From the thermograms, glass transition temperature (T_g), melting
 233 temperature (T_m), enthalpy of fusion (ΔH_m), and enthalpy of cold-crystallization (ΔH_{cc}) were
 234 determined. The crystallinity ($X\%$) of plastics was calculated using the following formula:

$$X\% = \frac{\Delta H_m - \Delta H_{cc}}{\Delta H_f \cdot (1 - \alpha)} \cdot 100, \quad (1)$$

235 where α is the amount of the additive in the plastic. The melting enthalpy of 100% crystalline
 236 (ΔH_f) PLA is 93.0 J/g (**Battegazzore et al., 2011**) and 207.1 J/g for PP (**Wunderlich, 2015**).

237 *MFR* was measured using a CEAST 7027.000 (Instron, Norwood, Massachusetts,
 238 USA) instrument. Its operational settings were based on ISO 1133-2:2011 (ISO 1133-2:2011,
 239 2011). The test temperature was 190 °C and the nominal load was 2.16 kg.

240 Both DSC and *MFR* measurements were performed in triplicate.

241 **2.4. Migration Tests and Sample Preparation**

242 The plastic sheets were cut into 30×10×2 mm (height×width×thickness) test
 243 specimens with a table saw. The width, length, height, and weight of each specimen were
 244 measured before immersion with Vernier callipers. The initial weights (m_{dry}) were determined
 245 using a Mettler Toledo AJ100L (Mettler Toledo, Columbus, Ohio, USA) analytical balance.
 246 The measured specimens were placed into 40 mL glass vials before adding pre-heated (40 °C)

247 food simulants (isooctane or ethanol 95 v/v%). For the migration experiments, the surface and
248 food simulant mass ratio recommended by Commission Regulation (EU) 10/2011
249 **(Commission Regulation (EU) 10/2011, 2011)** (supposing that cubic packaging with 6 dm²
250 surface contains 1 kg food or food simulant) was employed, i.e. 0.6 cm²/g food simulant.
251 Therefore, either 18 mL isooctane or 16 mL ethanol 95 v/v% was used. Samples were stored
252 at 40 °C in a POL-EKO ST2 laboratory incubator (Pol-Eko-Aparatura, Wodzisław Śląski,
253 Poland). The contact times for the kinetic studies were the following: 5 min, 30 min, 1 h, 2 h,
254 6 h, 12 h, 1 d, 2 d, 3 d, 4 d, 5 d, 6 d, 7 d, 8 d, 9 d, 10 d, 11 d, 12 d, 13 d. For each sampling
255 time, five parallel samples were prepared. After the defined contact times, the sample vials
256 were removed from the incubator for immediate preparation. The weight of swelled plastic
257 specimens (m_{swelled}) was measured after gentle wiping with a piece of blotting paper. When
258 the concentration of a migrated compound proved to be below or above the calibration range,
259 preconcentration or dilution was necessary (details are listed in *Supp. Inf. Table 2*). Mirex
260 served both as an evaporation and injection standard (ISTD). For enrichment, evaporation
261 under a nitrogen (purity: 4.5, Messer Hungarogáz Kft., Budapest, Hungary) stream was
262 applied. In these cases, mirex was added before the evaporation. The other samples were
263 spiked with ISTD solution before injection into GC-EI-QMS. Eventually, every sample
264 contained 10 mg/L mirex.

265 **2.5. GC-EI-QMS Analysis**

266 The quantitative analysis was performed using an Agilent 7890A gas chromatograph
267 (Agilent Technologies, Santa Clara, California, USA) equipped with a split/splitless inlet and
268 a 7683B autosampler coupled with an Agilent 5975C Inert XL MSD Mass Spectrometer with
269 an electron impact ion source, quadrupole analyzer, and triple-axis detector (Agilent
270 Technologies, Santa Clara, California, USA).

271 The samples were injected in split mode at a ratio of 1:10. The inlet temperature was
272 280 °C. The injection volume was 1 µL. A J&W DB-5MS ultra inert (Agilent Technologies,
273 Santa Clara, California, USA) capillary column was used with dimensions of 30 m × 0.25 mm
274 I.D. × 0.25 µm film thickness. The carrier gas was helium (purity: 5.0, Messer Hungarogáz
275 Kft., Budapest, Hungary) with a flow rate of 2.0 mL/min. The oven temperature was 100 °C
276 initially, then it was raised to 250 °C, at a rate of 30 °C/min. This temperature was maintained
277 for 4.5 min, then increased to 320 °C for 2.3 min at a rate of 30 °C/min. The final temperature
278 was maintained for 4 min. The electron impact (EI) ion source of the mass spectrometer was
279 applied with 70 eV ionization energy. The temperature of the ion source was 230 °C and the

280 quadrupole analyzer operated at 150 °C. The mass spectrometer was tuned with
 281 perfluorotributylamine (PFTBA, CAS: 311-89-7). For the quantitative analysis, single ion
 282 monitoring (SIM) mode was used. The qualifier and quantifier ions of target compounds are
 283 summarized in *Table 1*. The GC-EI-QMS was controlled using Agilent MSD ChemStation
 284 (E.02.02) software.

285 **2.6. Data Evaluation**

286 *2.6.1. Swelling degree*

287 From the mass of the initial (m_{dry}) and swelled (m_{swelled}) plastic specimen, the swelling
 288 degree ($SD\%$) can typically be determined using the following formula:

$$SD\% = \frac{m_{\text{swelled}} - m_{\text{dry}}}{m_{\text{dry}}} \cdot 100. \quad (2)$$

289 But the migration of additives causes a considerable decrease in the weight of the specimen,
 290 so it was decided that the adjusted swelling degree ($ASD\%$) should be calculated instead:

$$ASD\% = \frac{(m_{\text{swelled}} + c_{V,\text{mig},i} \cdot V_{\text{simulant}}) - m_{\text{dry}}}{m_{\text{dry}}} \cdot 100, \quad (3)$$

291 where $c_{V,\text{mig},i}$ is the mass concentration of i additive (mass of migrated i additive normalized to
 292 the volume of food simulant) and V_{simulant} is the volume of the food simulant. To investigate
 293 the swelling kinetic, $ASD\%$ was plotted as the function of contact time.

294 *2.6.2. Surface normalized concentration of the migrant*

295 Based on the measured dimensions (length, width, and height), the surface area of
 296 each specimen (A_{specimen}) was calculated. The results of quantitative analysis with GC-EI-
 297 QMS give information about the mass concentration of additive i in the food simulant
 298 ($c_{V,\text{mig},i}$). To consider the slight differences in the size of the test specimens, the surface
 299 normalized concentration of the migrants ($c_{A,\text{mig},i}$) was calculated from $c_{V,\text{mig},i}$:

$$c_{A,\text{mig},i} = \frac{c_{V,\text{mig},i} \cdot V_{\text{simulant}}}{A_{\text{specimen}}}. \quad (4)$$

300 On the migration kinetic curves, $c_{A,\text{mig},i}$ was plotted as the function of contact time. The extent
 301 of migration was characterized by the maximum value of $c_{A,\text{mig},i}$ for all cases, regardless of the
 302 presence or lack of a steady-state at the end of the migration experiment.

303 *2.6.3. Pearson's correlation test*

304 The supposed relationship between the swelling of the plastic and the additive
305 migration was investigated using *Pearson's* linear correlation test. Therefore, *ASD%* was
306 plotted as the function of $c_{A,mig,i}$, and *Pearson's* correlation coefficient (*PCC*) was calculated
307 using OriginPro 2018 (OriginLab Corporation, Northampton, Massachusetts, USA). When
308 the *PCC* value was above 0.9000, a strong correlation was assumed between *ASD%* and
309 $c_{A,mig,i}$.

Journal Pre-proof

310 2.6.4. Empirical semivariogram

311 Empirical semivariograms were calculated and plotted to assess the temporal
 312 autocorrelation structure of the concentrations of migrants and swelling degrees. **Kovács et**
 313 **al. (2012)** give a description of the variogram in which $Z(x)$ and $Z(x+h)$ represent two of the
 314 values measured for a particular parameter, and these two are at a distance h from each other.
 315 The distance h might be distance in time or in space. Proceeding from this, a value for the
 316 variance of the difference of $Z(x)$ and $Z(x+h)$ can be found, thus:

$$D^2[Z(x) - Z(x + h)] = D^2[Z(x)] + D^2[Z(x + h)] - 2cov[Z(x), Z(x + h)]. \quad (5)$$

317 Furthermore, if it is the case that the samples under consideration derive from the same
 318 population, then the following assumption may be made

$$D^2[Z(x)] = D^2[Z(x + h)], \quad (6)$$

319 and therefore

$$D^2[Z(x) - Z(x + h)] = 2D^2[Z(x)] - 2cov[Z(x), Z(x + h)] = 2\gamma(h) \quad (7)$$

320 The function expressed by $2\gamma(h)$ is the parameter's variogram, and from this, $\gamma(h)$ then
 321 represents its semivariogram. With the use of simplified notation

$$D^2[Z(x)] = D^2(x), \quad (8)$$

322 and

$$cov[Z(x), Z(x + h)] = g(h), \quad (9)$$

323 so

$$\gamma(h) = D^2(x) - g(h). \quad (10)$$

324 It is then possible to use the Matheron algorithm (**Matheron, 1965**) to calculate the empirical
 325 semivariogram

$$\gamma(h) = \frac{1}{2N(h)} \sum_{i=1}^{N(h)} [Z(x_i) - Z(x_i + h)]^2, \quad (11)$$

326 in which $N(h)$ is the number of pairs to be found within a lag interval h .

327 In this study, $Z(x)$ corresponds to the value of the parameter measured (e.g. $ASD\%$, $c_{A,mig,i}$) in
 328 time t and h to the time interval.

329 Of the semivariograms thus obtained, four types can be distinguished:

- 330 a) When the semivariogram increases continuously over the distance (be it time
331 or space) examined. In this case, the given process does not reach a steady-
332 state.
- 333 b) When the values of the empirical semivariogram fluctuate randomly around a
334 constant after the initial rise. In general, the value at which this occurs on the
335 vertical axis is called a *sill*. On the horizontal axis, it is called range. Since in
336 the present work variography is applied to kinetic curves, these range values
337 specify the starting points (in time) of the steady-state.
- 338 c) When the empirical semivariogram on the vertical axis does not start from the
339 origin, or the initial ascending part of the curve is missing, so the points of the
340 semivariogram fluctuate around the variance, a nugget-effect type variogram is
341 obtained. It should be noted that this effect may result from inadequate
342 sampling or measurement errors (**Hatvani et al., 2012**).
- 343 d) When the increase ends with variation around a constant, and this is repeated a
344 number of times, i.e. multiple ranges can be determined. This type of
345 semivariogram is called a nested semivariogram. It indicates that more than
346 one process has an influence on the variation of the data.

347 2.6.5. Analysis of variance (ANOVA)

348 The significance of differences was tested using ANOVA. The normal distribution of the
349 data was verified using the Shapiro-Wilk test (**Shapiro & Wilk, 1965**), the homoscedasticity
350 assumption was assessed by Bartlett's test. Due to the absence of homoscedasticity, Welch's
351 ANOVA was used, after which the Games-Howell *post-hoc* test was applied to compare all
352 possible pairs of additives (**Welch, 1951**). In the significance tests the maximum migrated
353 concentrations were compared for each of the PP and PLA samples. The same analysis was
354 performed with adjusted swelling degree data.

355 3. Results and discussion

356 3.1. Mechanical and thermal properties of produced plastics

357 The main mechanical and thermal properties of the plastics examined are summarized
358 in **Table 2**. *MFR* gives information about the flow properties of plastics, indirectly about their
359 molecular weight and dynamic viscosity in a molded state. The presence of a plasticizer in

360 PLA moderately influences the mechanical and thermal properties. PLAs containing TBAC or
361 TOTM have an increased *MFR* value compared to the reference plastic. Plasticizers also
362 change the glass transition temperature (T_g) by slightly decreasing it. In the first heat cycle in
363 the DSC analysis of PLA, the exotherm peak of cold-crystallization appears: T_{cc} of PLA
364 reference was 95.3 ± 0.3 °C, which fell to 86.3 ± 0.3 °C and 81.0 ± 0.1 °C due to TBAC and
365 TOTM, respectively. Some increase in the *MFR* value can be observed for BHT and Uvinul
366 3039 as well, but the other parameters show no distinct tendencies. Compoundation of PP
367 with additives (besides the Irgafos 168 that it originally contained) resulted in the increase in
368 *MFR*, irrespective of the function of additives. Otherwise, plastic additives at this level of
369 concentration hardly influence the thermal and mechanical properties of PP.

370 **3.2. Swelling of PLA and PP in isooctane and ethanol 95 v/v%**

371 *3.2.1. The effect of food simulant on swelling*

372 Even though isooctane and ethanol 95 v/v% are both commonly used as solvents to
373 substitute fatty food in migration tests, their physical-chemical characteristics differ
374 considerably. The difference can be observed in their ability to swell PP and PLA, as well.
375 **Figures 1.A and 1.C** show the swelling kinetic curves of the reference PLA (no additive) and
376 PP (with only Irgafos 168) samples, respectively.

377 The swelling of PLA in isooctane was negligible. Moreover, a slight but
378 unquestionable mass reduction was observed. Since this plastic did not contain any plastic
379 additive, this weight reduction cannot be explained by the migration of any substance. It
380 might be supposed that the decrease is the result of polymer degradation or solubilization. The
381 non-swelling effect of isooctane on PLA was also reported by **Sato et al. (2012)**, however the
382 solubility test they performed lasted only for 24 hours, and the contact temperature was only
383 35 °C.

384 Ethanol molecules are smaller than isooctane molecules and their polarity is closer to
385 that of PLA. Consequently, PLA swelling in ethanol 95 v/v% shows a different pattern. In this
386 case, in the thirteen days of the experiment, the swelling could not reach a lasting steady-state.
387 As the semivariogram in **Figure 1.B** shows the increase of the *ASD%* came to a short halt at
388 112 h, but then it continued without reaching any further steady-states. The maximum value
389 of *ASD%* (equal to *SD%* in this case) was $2.8 \pm 0.03\%$. Comparing this result to the work of
390 **Iñiguez-Franco et al. (2012)**, the notable effect of test specimen thickness on swelling can

391 be seen: they found that neat PLA film (with $27.9 \pm 9.9 \mu\text{m}$ thickness) reached swelling
392 equilibrium almost immediately with 6% ethanol sorption.

393 PP swells in both food simulants, however; due to its non-polar character, the
394 absorption of isooctane is more than one order of magnitude higher than that of ethanol. In
395 isooctane, the *ASD%* increases up to 165 h (based on its empirical semivariogram), at which
396 point a long-lasting steady-state starts at $8.9 \pm 0.15\%$. On the other hand, the swelling of PP in
397 ethanol 95 v/v% shows an unconventional pattern (**Figure 1.D**). After the initial increase of
398 *ASD%* a steady-state starts to form at 68 h, but instead of stabilizing permanently, the *ASD%*
399 starts to increase again to reach a second plateau at $0.24 \pm 0.01\%$, starting at 210 h. This
400 results in a nested semivariogram, and this behaviour suggests that the swelling advances
401 layer by layer, in accordance with the fact that polymer chain orientation varies along the
402 cross-section of test specimens. This heterogeneity in chain orientation is the result of
403 fountain flow in the injection molding process.

404 3.2.2. The effect of plastic additive's function on swelling

405 The kinetic curves of the swelling of the various PLA samples in ethanol 95 v/v% and
406 that of PP samples in isooctane – i.e. the solvent having a stronger swelling effect – are
407 presented in **Figures 2.A** and **2.B**. As expected, they show that plasticizers (TBAC and
408 TOTM) promote the swelling of both polymers. The maximum values of *ASD%* in the case of
409 PLA with no additive (reference), PLA–BHT, PLA–Ionox 220, and PLA–Uvinul 3039 are
410 between $2.8 \pm 0.03\%$ and $3.1 \pm 0.03\%$ in ethanol 95 v/v%. The statistical analysis proved that
411 there is no significant difference ($\alpha=0.05$) in the swelling of neat and antioxidant or UV
412 stabilizer spiked PLA, even though the *MFR* values of the PLA–BHT and PLA–Uvinul 3039
413 plastics are moderately elevated compared to the reference PLA. Meanwhile, the maximum
414 *ASD%* of PLA–TBAC and PLA–TOTM are $6.4 \pm 0.10\%$ and $4.3 \pm 0.23\%$, respectively. This
415 increase in the *ASD%* values of the two plasticizer-spiked PLAs is a result of the polymer
416 chain mobilizing effect of these additives.

417 The *ASD%* values for PP in isooctane at the end of the experiment for the plastics with
418 various additives fall within a narrow range ($8.8 \pm 0.08\%$ – $10.7 \pm 0.10\%$). However, the
419 statistical analysis revealed significant difference between PP with stabilizers and PP with
420 plasticizers. The plasticizing effect which facilitates easier swelling is even more apparent in
421 the slopes of the kinetic curves in the first 4 days of the experiments. Due to the faster
422 swelling, PP–TBAC and PP–TOTM reaches the steady-state at 44 h and 60 h, respectively.
423 Whereas, the samples without plasticizer took about 113–167 h to reach the final degree of

424 swelling. These results imply that the *ASD%* of PLA samples may eventually rise to a similar
425 value, too. But 13 days' contact time was clearly not enough to reach the equilibrium of the
426 PLA–ethanol system.

427 **3.3 Migration of additives**

428 *3.3.1. Migration in different polymer-solvent systems*

429 The surface normalized concentrations of the migrated additives as a function of time
430 provided different patterns for each of the polymer–food simulant pairs. In all cases,
431 significant differences ($\alpha=0.05$) were found using Welch's ANOVA among the maximum of
432 migrated concentrations (see **Table 3**). Furthermore, the significant difference for all possible
433 pairs was confirmed using the post-hoc test. As an example, both the swelling and migration
434 kinetic curves of the polymers containing TBAC are presented in **Figure 3**, whereas **Table 3**
435 lists the maximum observed concentrations of every additive. Isooctane does not swell PLA,
436 consequently, the additives appearing in the solvent within the 13 days come from the surface
437 layer of the plastic. Thus, the concentrations in the isooctane phase remain so low that their
438 measurement could be carried out only with a relatively high degree of uncertainty.
439 Furthermore, the mass transfer from the surface is prompt. As a result of these two factors,
440 nugget-effect type semivariograms were obtained for all additives in the PLA–isooctane
441 system.

442 In the PLA–ethanol systems for all additives, the maximum of the surface normalized
443 concentrations was three orders of magnitude higher. Within the 13 days of the experiments,
444 equilibrium could not be reached for any of the additives. Both the swelling and the migration
445 curves show an indisputably increasing trend, even though the rate of the increase is not
446 constant: at least one short halt can be detected in all cases.

447 For PP, the situation is reversed. Ethanol can only slightly penetrate PP, but isooctane
448 swells it considerably. Consequently, migration of the additives studied from PP into
449 isooctane gave typically concentrations in the solvent phase one order of magnitude higher
450 than that into ethanol 95 v/v%. With the exception of BHT, the migration curves in the PP–
451 isooctane systems showed a dynamically increasing initial part, which between 63 h and 255
452 h turned into a presumably long-lasting steady-state. But the migration of BHT into isooctane
453 slowed down for a short while and then increased again to reach a lasting steady-state at
454 163 h. Such changes in the rate of increase of the migrated concentrations were, however,
455 much more characteristic of the PP–ethanol systems. These halts and plateaus in the increase
456 of surface normalized concentrations in the liquid phase of the PLA–ethanol and the PP–

457 ethanol systems indicate that not only the swelling, but also the migration proceeds layer by
458 layer. The observation of this phenomenon was facilitated by the use of unusually thick test
459 specimens.

460 The effect of swelling on the migrant concentrations can be observed clearly on the
461 maximum values of surface normalized concentrations as well. For all additives, the highest
462 concentrations were observed when PP was in contact with isooctane, that is, where the
463 swelling was the most intense. A similar observation was made by **Alin & Hakkarainen**
464 **(2010)**, who investigated the migration of two antioxidants (Irganox 1010 and Irgafos 168)
465 from PP-based FCP into various food simulants by microwave irradiation. In their research
466 they found that the amount of Irganox 1010 and Irgafos 168 was approximately 40 and 20
467 times higher in isooctane than in ethanol 95 v/v%, respectively (**Alin & Hakkarainen, 2010**).

468 Isooctane with PLA provided the lowest concentrations, in agreement with the lack of
469 swelling. Ethanol was absorbed by both PLA and PP, but not to the same extent. The ASD%
470 values for PLA samples were about one order of magnitude higher than those for the PP
471 samples. Accordingly, for every additive, the concentrations in ethanol 95 v/v% were higher
472 when they migrated from the PLA.

473 3.3.2. Molecular weight of additives and migration

474 For the comparison of the observed concentrations in the food simulants across the
475 different additives, one must take into consideration the fact that for the preparation of the
476 plastics, the additives were applied in different mass ratios. **Figure 4** shows the surface
477 normalized concentrations divided by the applied mass ratios for both PLA and PP.

478 For the stabilizer additives (BHT, Ionox 220, Uvinul 3039, and Irgafos 168), a clear tendency
479 can be observed in the migration concentrations: as the molecular weights of the additives
480 increase, the migrated concentrations decrease. The diffusion of chemical compounds is an
481 essential part of migration from plastics which thus depends directly on the hydrodynamic or
482 Stokes radius of the migrating molecule at a given temperature and hence, indirectly, on its
483 molecular weight. Beyond molecular weight, the size and shape of the migrating compound,
484 and its affinity to the formation of intermolecular interactions can be essential in the process
485 of migration. **Samsudin et al. (2014)** in their work compared their results (for astaxanthin
486 release) with previous antioxidant migration studies from PLA. They noticed that the
487 diffusion coefficient of BHT (**Ortiz-Vazquez et al., 2011**) is at least twice as high as any
488 other antioxidant's. The presumed explanation for the higher migration rate was the BHT
489 molecule's non-bulky structure, compared to the other compounds examined. **Samsudin et al.**

490 (2014) also considered the theory of **Iñiguez-Franco et al. (2012)** concerning the number of
491 hydroxyl groups in the migrating compound molecule, which speculates that the presence of
492 this functional group decreases the release rate.

493 The pattern expected on the basis of the additives' molecular weight is disturbed by
494 the plasticizers. According to the molecular weight of the additives, the expected order of
495 maximum migration concentration would be: Irgafos 168 (PP only) < TOTM < Ionox 220 <
496 TBAC < Uvinul 3039 < BHT. However, in PLA the order was: Ionox 220 < TOTM < Uvinul
497 3039 < BHT < TBAC; while in PP it was: Irgafos 168 < Ionox 220 < Uvinul 3039 < BHT <
498 TOTM < TBAC. The reason of the change is the chain mobilizing effect of the plasticizers.

499 TBAC facilitated its own diffusion among the polymer chains of both PLA and PP to
500 such an extent that its migration concentrations went higher than that of all the smaller
501 stabilizer additives (BHT, Ionox 220 and Uvinul 3039). In the PP–isooctane system, the same
502 happens for TOTM, hence its curve on **Figure 4** closely approaches that of TBAC instead of
503 Irgafos 168. But the plasticizing effect of TOTM in PLA was not as intense as that of TBAC.
504 As **Figure 2.A** shows, the swelling of PLA–TOTM is approximately in the middle between
505 the PLA–TBAC and the other PLA-based plastics. This is in accordance with the picture in
506 **Figure 4**, in which its curve moves just a bit above that of Ionox 220 even though its higher
507 molecular weight would suggest otherwise. On the other hand, the plasticizing effect of
508 TOTM was enough for a moderate enhancement of the swelling, which in turn was able to
509 facilitate its migration somewhat over the migration of the next additive in line. But this effect
510 was not strong enough to elevate this migration to the level of the smaller additives, let alone
511 TBAC.

512 **3.4. Correlation between swelling degree and migrated concentration of additives**

513 Both swelling and migration kinetic curves displayed various shapes. As detailed in
514 the previous sections, there were occasions when the change in the relevant parameter was
515 small compared to the degree of uncertainty in its measurement. In the case of the most
516 intense swellings and migrations, the curves reached a steady-state after a consistent increase
517 at the beginning of the experiments. A stepwise increase was also often observed. Even amid
518 this great variety, the corresponding swelling and migration curves always followed the same
519 pattern. To demonstrate that the similarity in the shapes of the curves is a result of a strong
520 relationship between the two processes, $ASD\%$ and $c_{A,mig,i}$ values were correlated. Since the
521 isooctane absorption of PLA was negligible, these cases were not considered. For all the other
522 polymer–additive–solvent systems the obtained *Pearson's* correlation coefficients showed a

523 strong linear correlation, as they ranged between 0.9664 and 0.9924, except for Uvinul 3039
524 in PP–isooctane, for which the value was 0.9134.

525 **Figure 5** demonstrates the relation between the swelling and migration curves of the
526 PLA–Uvinul 3039 (**Figure 5.A**) and the PP–BHT (**Figure 5.B**) samples in contact with
527 ethanol 95 v/v%. Their respective semivariograms are also shown. Both of these curves show
528 stepwise processes. In the case of PLA–Uvinul 3039, neither the swelling nor the migration
529 could reach steady-state. Still, short halts in the increase of the respective parameter can be
530 observed. The presence of these is confirmed for both curves by their nested semivariograms.
531 Moreover, with the help of the variograms, the starting points of these halts can be identified.
532 As **Figure 5.A** shows, in this case starting points on the two curves follow each other closely,
533 there is no significant difference between the time pairs.

534 **Figure 5.B** also shows a stepwise increase for both swelling and migration for the PP–
535 BHT samples. In this case, however, the starting points in the migration curve are
536 considerably delayed with respect to those in the swelling curve. As a result, only two starting
537 points can be detected in the migration curve within the 13 day timeframe of the experiment,
538 whereas the swelling curve has three. It is safe to assume that over the 13 days, a further
539 increase in the concentration of BHT in the ethanol 95 v/v% could be observed.

540 The starting points identified by the semivariograms for the other polymer–additive
541 pairs are listed in **Table 4**. Most of the data follow one or other of the above-described
542 patterns: practically equal starting points or considerably delayed migration. In some cases
543 (e.g. PP–Uvinul 3039 in ethanol 95 v/v%), the delay at the first detected point is negligible,
544 but by the second plateau, the delay becomes obvious. Either way, the migration always
545 follows the swelling, even if closely. The only exception seems to be Ionox 220 migrating
546 from PLA to ethanol 95 v/v%. In this case, the first halt in the migration is so short that the
547 corresponding halt in the swelling curve could only be detected after increasing the frequency
548 of the sampling. Unfortunately, the presence and the extent of the delays shows no apparent
549 pattern. Consequently, the time necessary to reach a steady-state on the migration curve
550 cannot be predicted on the basis of the swelling curve.

551 4. Conclusions

552 In the present work, the time dependence of the migration of commonly used plastic
553 additives from polylactic acid (PLA) and polypropylene (PP) to ethanol 95 v/v% and
554 isooctane was investigated in 13 day long experiments. Alongside the measurement of the
555 concentration of the additives in these food simulants, the swelling of the test specimens was
556 followed. As expected, a strong correlation was observed between the two processes.

557 PLA cannot be swelled by isooctane, but it is penetrated by ethanol, whereas PP is
558 swelled to a great degree by isooctane and only slightly by ethanol. For all polymer-food
559 simulant pairs, where swelling can be observed, the addition of plasticizers increased the rate
560 and degree of swelling, though this change had a smaller effect than changing the polymer or
561 the food simulant in the experimental setting.

562 Both for swelling and migration, a stepwise increase in the relevant parameter was
563 observed. Short halts in the increase were characteristic rather of the PLA–ethanol systems,
564 whereas clear plateaus formed when PP was in contact with ethanol 95 v/v%. The kinetic
565 curves of the PP samples in isooctane were, in general, more regular: they consisted of a
566 dynamically increasing initial part, which turned into a lasting steady-state.

567 Regardless of the shape of the kinetic curves, for all additives the greater the swelling,
568 the higher migration concentrations observed. This relation between swelling and migration
569 has an important implication. Whenever isooctane and ethanol 95 v/v% as simulants are used
570 for fatty food instead of vegetable oil, the decision on the compliance of the tested plastic
571 must be based on the highest observed migration concentrations to ensure food safety. If the
572 migration tests are performed only in the solvent that provides these higher concentrations,
573 the number of experiments can be about half of what would otherwise be allotted. The results
574 presented here suggest that for additives that are well soluble in both simulants, the solvent
575 that can better penetrate the plastic should be used. On the other hand, using a solvent that
576 swells the polymer much better than vegetable oil will probably result in the extreme
577 overestimation of the migration.

578 The diffusion of the additives is an essential part of their migration to food simulants.
579 So, the hydrodynamic or Stokes radius of the migrating molecule and thus, indirectly, the
580 molecular weight may be expected to influence the concentration of the migrants.
581 Accordingly, the migration of stabilizers from PLA to ethanol 95 v/v%, as well as from PP to
582 isooctane decreased with increasing molecular weight. But the migration of TBAC was
583 stronger in both cases, even though its molecular weight is bigger than that of BHT and

584 Uvinul 3039. This means that the promoting effect of plasticizing on swelling and thus
585 migration outweighed the demoting effect of the higher molecular mass.

586 The strong correlation between the swelling degree and migration concentrations was
587 confirmed by the fact that the values of *Pearson's* correlation coefficients were over 0.9100.
588 Furthermore, variography was successfully employed in the determination of the start of
589 plateaus on the kinetic curves. In the case of PLA–isooctane systems, nugget-effect type
590 empirical semivariograms were obtained due to the low level of migration and the
591 comparatively high uncertainty of the concentration results. But for all other cases, the
592 semivariograms could objectively highlight the starting points of both short halts and
593 somewhat longer plateaus in the increase of either the swelling degree or the migrant
594 concentration. The result thus obtained unambiguously showed that migration, either closely
595 or loosely, nonetheless strictly follows the swelling even in the case of multiple-level curves.

596 All these results prove that the extent of the migration of a certain additive should not
597 be estimated solely on parameters characterizing the materials alone (additive, polymer and
598 food simulant). Rather, it is the interactions between these parameters, especially the
599 plasticizing effect of either the additive or the solvent, that are fundamental.

600 **Acknowledgement**

601 We are thankful to Wessling International Research and Education Center (WIREC)
602 for providing financial support, laboratory equipment, and materials for our research. The
603 authors gratefully acknowledge the helpful work of the technical staff of Budapest University
604 of Technology and Economics, Faculty of Mechanical Engineering, Department of Polymer
605 Engineering in the manufacture of plastic specimens. We are also thankful to BASF Hungary
606 Ltd. for donating Uvinul 3039.

607 This research program has been implemented with support provided by the National
608 Research, Development and Innovation Fund of Hungary, financed under project No. 128440
609 of the FK18 funding scheme and from the Hungarian Ministry of Human Capacities financed
610 under the ELTE Institutional Excellence Program (TKP2020-IKA-05). This work was
611 supported by the National Research, Development, and Innovation Office, Hungary (2019-
612 1.1.1-PIACI-KFI-2019-00205, 2017-2.3.7-TÉT-IN-2017-00049, OTKA FK134336). The
613 research reported in this paper and carried out at BME is supported by the NRDIFund
614 (TKP2020 NC, Grant No. BME-NCS) based on the charter of bolster issued by the NRDIFund
615 Office under the auspices of the Ministry for Innovation and Technology. This paper was
616 supported by the János Bolyai Research Scholarship of the Hungarian Academy of Sciences.
617 The research was supported by the ÚNKP-20-5 New National Excellence Program of the
618 Ministry for Innovation and Technology from the source of the National Research,
619 Development and Innovation Fund. This publication was supported by the Italian-Hungarian
620 bilateral agreement (grant number NKM 73/2019) of the Hungarian Academy of Sciences.

- 621 **CRedit (Contributor Roles Taxonomy) authorship contribution statement**
622
- 623 **Csaba Kirchkeszner:** conceptualization, design and conduct the experiments, data evaluation
624 and visualization, formal analysis, writing – original draft
- 625 **Noémi Petrovics:** conceptualization, design and conduct the experiments, data evaluation and
626 visualization, formal analysis, writing – original draft
- 627 **Tamás Tábi:** production and analysis of plastics, data interpretation, writing – review &
628 editing, funding acquisition
- 629 **Norbert Magyar:** data visualization, formal analysis, writing – review & editing
- 630 **József Kovács:** data visualization, formal analysis, writing – review & editing, funding
631 acquisition
- 632 **Bálint Sámuel Szabó:** writing – review & editing, conceptualization
- 633 **Zoltán Nyiri:** writing – review & editing, conceptualization
- 634 **Zsuzsanna Eke:** conceptualization, supervision, writing – review & editing, funding
635 acquisition

636 **References**

- 637 Alin, J., & Hakkarainen, M. (2010). Type of polypropylene material significantly influences
638 the migration of antioxidants from polymer packaging to food simulants during
639 microwave heating. *Journal of Applied Polymer Science*, *118*(2), 1084–1093.
640 <https://doi.org/10.1002/app.32472>
- 641 Aznar, M., Ubeda, S., Dreolin, N., & Nerín, C. (2019). Determination of non-volatile
642 components of a biodegradable food packaging material based on polyester and
643 polylactic acid (PLA) and its migration to food simulants. *Journal of Chromatography A*,
644 *1583*, 1–8. <https://doi.org/10.1016/j.chroma.2018.10.055>
- 645 Battegazzore, D., Bocchini, S., & Frache, A. (2011). Crystallization kinetics of poly(lactic
646 acid)-talc composites. *Express Polymer Letters*, *5*(10), 849–858.
647 <https://doi.org/10.3144/expresspolymlett.2011.84>
- 648 Bodai, Z., Kirchkeszner, C., Novák, M., Nyiri, Z., Kovács, J., Magyar, N., Iván, B., Rikker,
649 T., & Eke, Z. (2015). Migration of Tinuvin P and Irganox 3114 into milk and the
650 corresponding authorised food simulant. *Food Additives and Contaminants - Part A*
651 *Chemistry, Analysis, Control, Exposure and Risk Assessment*, *32*(8), 1358–1366.
652 <https://doi.org/10.1080/19440049.2015.1055523>
- 653 Chang, Y., Kang, K., Park, S. J., Choi, J. C., Kim, M. K., & Han, J. (2019). Experimental and
654 theoretical study of polypropylene: Antioxidant migration with different food simulants
655 and temperatures. *Journal of Food Engineering*, *244*(February 2018), 142–149.
656 <https://doi.org/10.1016/j.jfoodeng.2018.09.028>
- 657 European Commission (2011). Plastic materials and articles intended to come into contact
658 with food. *European Commission Regulation No 10/2011 EC*. Available at: [https://eur-
659 lex.europa.eu/legal-content/EN/TXT/?uri=CELEX%3A02011R0010-20200923](https://eur-lex.europa.eu/legal-content/EN/TXT/?uri=CELEX%3A02011R0010-20200923)
- 660 Feigenbaum, A. E., Riquet, A. M., & Scholler, D. (2000). Fatty food simulants: Solvents to
661 mimic the behavior of fats in contact with packaging plastics. In *ACS Symposium Series*
662 (Vol. 753, Issue 1, pp. 71–81). <https://doi.org/10.1021/bk-2000-0753.ch007>
- 663 Garde, J. A., Catalá, R., Gavara, R., & Hernandez, R. J. (2001). Characterizing the migration
664 of antioxidants from polypropylene into fatty food simulants. *Food Additives and*
665 *Contaminants*, *18*(8), 750–762. <https://doi.org/10.1080/02652030116713>

- 666 Gavriil, G., Kanavouras, A., & Coutelieris, F. A. (2018). Food-packaging migration models:
667 A critical discussion. *Critical Reviews in Food Science and Nutrition*, 58(13), 2262–
668 2272. <https://doi.org/10.1080/10408398.2017.1317630>
- 669 Hatvani, I., Kovács, J., & Korponai, J. (2012). Mintavételezési gyakoriság optimalizálása
670 variogram függvényrel a Kis-Balaton Vízvédelmi Rendszer példáján. *Természetvédelmi*
671 *Közlemények*, 18(Pomogyi 1991), 202–210.
- 672 Hatvani, G., Kirschner, A. K. T., Farnleitner, A. H., Tanos, P., & Herzig, A. (2018). Hotspots
673 and main drivers of fecal pollution in Neusiedler See, a large shallow lake in Central
674 Europe. *Environmental Science and Pollution Research*, 25(29), 28884–28898.
675 <https://doi.org/10.1007/s11356-018-2783-7>
- 676 Hatvani, G., Erdélyi, D., Vreča, P., & Kern, Z. (2020). Analysis of the spatial distribution of
677 stable oxygen and hydrogen isotopes in precipitation across the Iberian Peninsula. *Water*
678 *(Switzerland)*, 12(2). <https://doi.org/10.3390/w12020481>
- 679 Hatvani, G., Leuenberger, M., Kohán, B., & Kern, Z. (2017). Geostatistical analysis and
680 isoscape of ice core derived water stable isotope records in an Antarctic macro region.
681 *Polar Science*, 13, 23–32. <https://doi.org/10.1016/j.polar.2017.04.001>
- 682 Hatvani, G., Magyar, N., Zessner, M., Kovács, J., & Blaschke, A. P. (2014). Die Europäische
683 Wasserrahmenrichtlinie: Kann man aus den Grundwassermessdaten mehr Informationen
684 gewinnen? Eine Fallstudie im Seewinkel, Burgenland, Österreich. *Hydrogeology*
685 *Journal*, 22(4), 779–794. <https://doi.org/10.1007/s10040-013-1093-x>
- 686 Iñiguez-Franco, F., Auras, R., Burgess, G., Holmes, D., Fang, X., Rubino, M., & Soto-
687 Valdez, H. (2016). Concurrent solvent induced crystallization and hydrolytic degradation
688 of PLA by water-ethanol solutions. *Polymer*, 99, 315–323.
689 <https://doi.org/10.1016/j.polymer.2016.07.018>
- 690 Iñiguez-Franco, F., Auras, R., Rubino, M., Dolan, K., Soto-Valdez, H., & Selke, S. (2017).
691 Effect of nanoparticles on the hydrolytic degradation of PLA-nanocomposites by water-
692 ethanol solutions. *Polymer Degradation and Stability*, 146, 287–297.
693 <https://doi.org/10.1016/j.polymdegradstab.2017.11.004>
- 694 Iñiguez-Franco, F., Soto-Valdez, H., Peralta, E., Ayala-Zavala, J. F., Auras, R., & Gámez-
695 Meza, N. (2012). Antioxidant activity and diffusion of catechin and epicatechin from

- 696 antioxidant active films made of poly(l-lactic acid). *Journal of Agricultural and Food*
697 *Chemistry*, 60(26), 6515–6523. <https://doi.org/10.1021/jf300668u>
- 698 ISO 1133-2:2011 (2011). *Plastics – Determination of the melt mass-flow rate (MFR) and melt*
699 *volume-flow rate (MVR) of thermoplastics – Part 2: Method for materials sensitive to*
700 *time-temperature history and/or moisture*. International Organization for
701 Standardization.
- 702 Jamshidian, M., Tehrany, E. A., & Desobry, S. (2012). Release of synthetic phenolic
703 antioxidants from extruded poly lactic acid (PLA) film. *Food Control*, 28(2), 445–455.
704 <https://doi.org/10.1016/j.foodcont.2012.05.005>
- 705 Jamshidian, M., Tehrany, E. A., & Desobry, S. (2013). Antioxidants Release from Solvent-
706 Cast PLA Film: Investigation of PLA Antioxidant-Active Packaging. *Food and*
707 *Bioprocess Technology*, 6(6), 1450–1463. <https://doi.org/10.1007/s11947-012-0830-9>
- 708 Kang, K., Chang, Y., Choi, J. C., Park, S. J., & Han, J. (2018). Migration Study of Butylated
709 Hydroxytoluene and Irganox 1010 from Polypropylene Treated with Severe Processing
710 Conditions. *Journal of Food Science*, 83(4), 1005–1010. [https://doi.org/10.1111/1750-](https://doi.org/10.1111/1750-3841.14104)
711 [3841.14104](https://doi.org/10.1111/1750-3841.14104)
- 712 Kern, Z., Erdelyi, D., Vreča, P., Krajcar Bronić, I., Forizs, I., Kandu, T., Štrok, M., Palcsu, L.,
713 Suveges, M., Czuppon, G., Kohan, B., & Hatvani, I. G. (2020). Isoscape of amount-
714 weighted annual mean precipitation tritium (3H) activity from 1976 to 2017 for the
715 Adriatic-Pannonian region - AP3H_v1 database. *Earth System Science Data*, 12(3),
716 2061–2073. <https://doi.org/10.5194/essd-12-2061-2020>
- 717 Kovács, J., Korponai, J., Székely Kovács, I., & Hatvani, I. G. (2012). Introducing sampling
718 frequency estimation using variograms in water research with the example of nutrient
719 loads in the Kis-Balaton Water Protection System (W Hungary). *Ecological*
720 *Engineering*, 42, 237–243. <https://doi.org/10.1016/j.ecoleng.2012.02.004>
- 721 Kuorwel, K. K., Cran, M. J., Sonneveld, K., Miltz, J., & Bigger, S. W. (2013). Migration of
722 antimicrobial agents from starch-based films into a food simulant. *LWT - Food Science*
723 *and Technology*, 50(2), 432–438. <https://doi.org/10.1016/j.lwt.2012.08.023>
- 724 Lu, W., Jiang, K., Chu, Z., Yuan, M., Tang, Z., & Qin, Y. Y. (2021). Changes of thermal
725 properties and microstructure of nano-ZnO/polylactic acid composite films during Zn

- 726 migration. *Packaging Technology and Science*, 34(1), 3–10.
727 <https://doi.org/10.1002/pts.2535>
- 728 Manzanarez-López, F., Soto-Valdez, H., Auras, R., & Peralta, E. (2011). Release of α -
729 Tocopherol from Poly(lactic acid) films, and its effect on the oxidative stability of
730 soybean oil. *Journal of Food Engineering*, 104(4), 508–517.
731 <https://doi.org/10.1016/j.jfoodeng.2010.12.029>
- 732 Mascheroni, E., Guillard, V., Nalin, F., Mora, L., & Piergiovanni, L. (2010). Diffusivity of
733 propolis compounds in Polylactic acid polymer for the development of anti-microbial
734 packaging films. *Journal of Food Engineering*, 98(3), 294–301.
735 <https://doi.org/10.1016/j.jfoodeng.2009.12.028>
- 736 Matheron, G. (1965). *JOURNAL DE LA SOCIÉTÉ STATISTIQUE DE PARIS Présentation*
737 *des variables régionalisées*. 107, 263–275.
- 738 Nasiri, A., Peyron, S., Gastaldi, E., & Gontard, N. (2016). Effect of nanoclay on the transfer
739 properties of immanent additives in food packages. *Journal of Materials Science*, 51(21),
740 9732–9748. <https://doi.org/10.1007/s10853-016-0208-x>
- 741 Ortiz-Vazquez, H., Shin, J., Soto-Valdez, H., Auras, R. (2011). Release of butylated
742 hydroxytoluene (BHT) from Poly(lactic acid) films. *Polymer Testing*, 30(5), 463–471.
743 <https://doi.org/10.1016/j.polymertesting.2011.03.006>
- 744 Ramos, M., Beltrán, A., Peltzer, M., Valente, A. J. M., & Garrigós, M. del C. (2014). Release
745 and antioxidant activity of carvacrol and thymol from polypropylene active packaging
746 films. *LWT - Food Science and Technology*, 58(2), 470–477.
747 <https://doi.org/10.1016/j.lwt.2014.04.019>
- 748 Samsudin, H., Auras, R., Mishra, D., Dolan, K., Burgess, G., Rubino, M., Selke, S., & Soto-
749 Valdez, H. (2018). Migration of antioxidants from polylactic acid films: A parameter
750 estimation approach and an overview of the current mass transfer models. *Food*
751 *Research International*, 103(July 2017), 515–528.
752 <https://doi.org/10.1016/j.foodres.2017.09.021>
- 753 Samsudin, H., Soto-Valdez, H., & Auras, R. (2014). Poly(lactic acid) film incorporated with
754 marigold flower extract (*Tagetes erecta*) intended for fatty-food application. *Food*
755 *Control*, 46, 55–66. <https://doi.org/10.1016/j.foodcont.2014.04.045>

- 756 Sato, S., Gondo, D., Wanda, T., Kanehashi, S., Nagai, K. (2012). Effects of various liquid
757 organic solvents on solvent-induced crystallization of amorphous poly(lactic acid) film.
758 *Journal of Applied Polymer Science*, 129(3), 1607–1617.
759 <https://doi.org/10.1002/app.38833>
- 760 Shapiro, S. S., & Wilk, M. B. (1965). *An Analysis of Variance Test for Normality (Complete*
761 *Samples)* (Vol. 52, Issue 3). <https://www.jstor.org/stable/2333709>
- 762 Trásy, B., Garamhegyi, T., Laczkó-Dobos, P., Kovács, J., & Hatvani, I. G. (2018).
763 Geostatistical screening of flood events in the groundwater levels of the diverted inner
764 delta of the Danube River: Implications for river bed clogging. *Open Geosciences*, 10(1),
765 64–78. <https://doi.org/10.1515/geo-2018-0006>
- 766 Vera, P., Canellas, E., & Nerín, C. (2018). Identification of non volatile migrant compounds
767 and NIAS in polypropylene films used as food packaging characterized by UPLC-
768 MS/QTOF. *Talanta*, 188, 750–762. <https://doi.org/10.1016/j.talanta.2018.06.022>
- 769 Welch, B. L. (1951). *On the Comparison of Several Mean Values: An Alternative Approach*
770 (Vol. 38, Issue 3).
- 771 Wunderlich, B. (2005). Structure and Properties of Materials. In B. Wunderlich (Ed.),
772 *Thermal Analysis of Polymeric Materials*, (pp. 512–516). Springer.
- 773 Yang, W., Fortunati, E., Dominici, F., Giovanale, G., Mazzaglia, A., Balestra, G. M., Kenny,
774 J. M., & Puglia, D. (2016). Effect of cellulose and lignin on disintegration, antimicrobial
775 and antioxidant properties of PLA active films. *International Journal of Biological*
776 *Macromolecules*, 89, 360–368. <https://doi.org/10.1016/j.ijbiomac.2016.04.068>
- 777
- 778

779 **Figure captions**

780 **Figure 1** Swelling kinetic curves of reference PLA (**1.A**) and PP (**1.C**) in isooctane and
781 ethanol 95 v/v%, and their empirical semivariograms in ethanol 95 v/v% (**1.B** for PLA and
782 **1.D** for PP)

783 **Figure 2** Swelling kinetic curves of PLA (**2.A**) in ethanol 95 v/v% and PP (**2.B**) in isooctane

784 **Figure 3** Migration and swelling of TBAC-compounded PLA (**3.A** and **3.B**) and PP (**3.C** and
785 **3.D**) in isooctane and ethanol 95 v/v%, respectively

786 **Figure 4** Surface normalized concentrations divided by the applied mass ratios of the
787 additives for PLA and PP in ethanol 95 v/v% and isooctane, respectively (Molecular weight
788 values: $M_{\text{BHT}} = 220.3$ g/mol, $M_{\text{Uvinul 3039}} = 361.5$ g/mol, $M_{\text{TBAC}} = 402.5$ g/mol, $M_{\text{IonoX 220}} =$
789 424.7 g/mol, $M_{\text{TOTM}} = 546.8$ g/mol, $M_{\text{Irgafos 168}} = 646.9$ g/mol)

790 **Figure 5** Relation between swelling and surface normalized concentrations in ethanol 95
791 v/v% for Uvinul 3039 from PLA (**5.A**) and BHT from PP (**5.B**)

792 **Table captions**

793 **Table 1** Retention time, qualifier and quantifier ions, *LLOQ* and recovery (at *LLOQ*) of target
794 compounds

795 **Table 2** Mechanical and thermal properties of the investigated plastic samples

796 **Table 3** Maximum surface normalized concentrations

797 **Table 4** Starting points of steady-states in the swelling and migration curves

Table 1 Retention time, qualifier and quantifier ions, *LLOQ* and recovery (at *LLOQ*) of target compounds

<i>Target Compounds</i>	<i>Retention time (min)</i>	<i>Quantifier ion (m/z)</i>	<i>Qualifier ions (m/z)</i>		<i>LLOQ*</i> (mg/L)		<i>Recovery at LLOQ (%)</i>	
					<i>Ethanol 95 v/v%</i>	<i>Isooctane</i>	<i>Ethanol 95 v/v%</i>	<i>Isooctane</i>
BHT	6.67	205	145	220	0.025	0.05	104.8	112.6
Ionox 220	12.62	409	367	424	0.5	0.5	97.3	119.6
Irgafos 168	16.81	441	147	308	0.5	0.1	101.6	112.9
Uvinul 3039	12.86	249	204	360	0.5	0.5	87.3	89.1
TBAC	9.48	185	259	129	0.1	0.1	119.9	81.6
TOTM	16.97	305	193	435	0.5	0.1	89.7	108.0
Mirex (ISTD)	12.33	272	237	332	–	–	–	–

**LLOQ*: lower limit of quantitation

Table 4 Starting points of steady-states in the swelling and migration curves

<i>Additives</i>	<i>Starting points of steady-states</i> (h)		
	<i>Swelling</i>	<i>Migration</i>	
<i>PLA-ethanol</i>	BHT	87; 165	87; 165
	Ionox 220	111; 191	70; 143; 193
	Uvinul 3039	63; 135; 261	68; 135; 260
	TBAC	112; 167	117; 237
	TOTM	73; 112; 162	93; 147; 212
<i>PP-ethanol</i>	BHT	87; 163; 260	115; 260
	Ionox 220	60; 167	163; 260
	Irgafos 168	68; 210	116; 238
	Uvinul 3039	93; 167	117; 233
	TBAC	67; 133; 207	73; 133; 207
	TOTM	117; 213	188
<i>PP-isooctane</i>	BHT	60; 113	87; 165
	Ionox 220	114	255
	Irgafos 168	165	208
	Uvinul 3039	167	167
	TBAC	44	63
	TOTM	60	115

Table 2 Mechanical and thermal properties of the investigated plastic samples

	<i>Additives</i>	<i>MFR</i> (g/10 min)	<i>T_g</i> (°C)	<i>T_m</i> (°C)	<i>ΔH_m</i> (J/g)	<i>T_{cc}</i> (°C)	<i>ΔH_{cc}</i> (J/g)	<i>X</i> (%)
2500HP PLA	Reference	3.2 ± 0.1	61.1 ± 0.1	175.8 ± 0.1	46.8 ± 1.0	95.3 ± 0.3	28.1 ± 1.1	20.1 ± 0.8
	BHT	5.1 ± 0.1	61.7 ± 0.1	175.6 ± 0.1	45.4 ± 0.7	90.7 ± 0.2	24.7 ± 0.6	22.5 ± 0.8
	Ionox 220	3.4 ± 0.1	61.2 ± 0.2	175.5 ± 0.0	46.4 ± 0.4	91.4 ± 0.2	24.7 ± 1.1	23.6 ± 1.4
	Uvinul 3039	5.4 ± 0.1	61.3 ± 0.2	175.3 ± 0.2	46.1 ± 1.0	90.9 ± 0.1	26.5 ± 0.8	21.2 ± 0.4
	TBAC	6.8 ± 0.2	55.8 ± 0.2	174.4 ± 0.0	41.2 ± 1.0	86.3 ± 0.3	21.3 ± 0.9	22.5 ± 2.2
	TOTM	6.5 ± 0.1	56.3 ± 0.1	174.4 ± 0.1	46.9 ± 1.6	81.0 ± 0.1	21.4 ± 0.3	28.9 ± 2.2
H145F PP	Reference*	9.8 ± 0.1	–	165.1 ± 0.1	81.5 ± 1.0	–	–	39.4 ± 0.5
	BHT	13.9 ± 0.1	–	164.5 ± 0.2	77.6 ± 1.4	–	–	37.5 ± 0.7
	Ionox 220	13.3 ± 0.1	–	164.6 ± 0.0	87.2 ± 1.9	–	–	42.1 ± 0.9
	Uvinul 3039	14.0 ± 0.1	–	164.8 ± 0.1	81.2 ± 0.7	–	–	39.2 ± 0.3
	TBAC	15.1 ± 0.1	–	163.6 ± 0.1	82.3 ± 1.0	–	–	39.8 ± 0.5
	TOTM	14.9 ± 0.2	–	164.1 ± 0.2	80.9 ± 2.6	–	–	39.0 ± 1.2

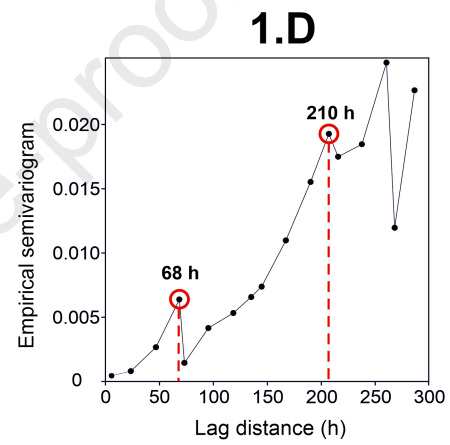
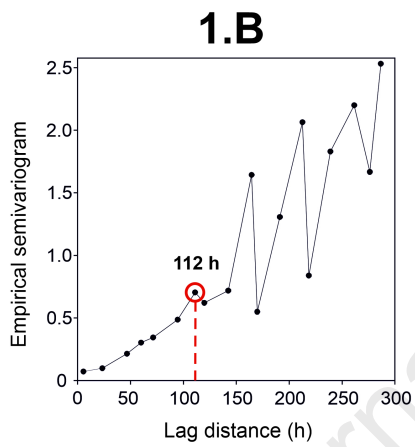
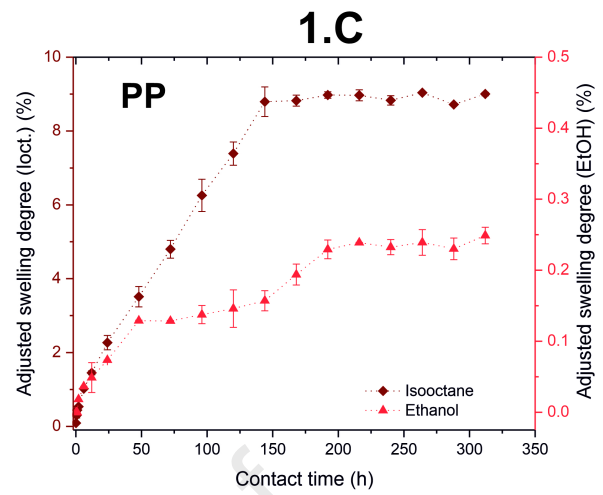
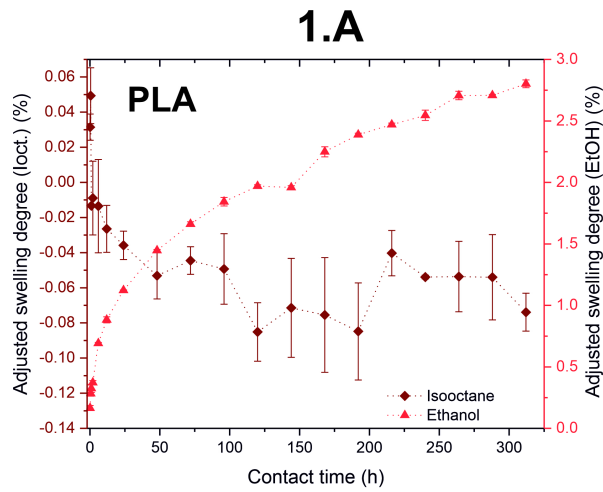
*It contained Irgafos 168 antioxidant.

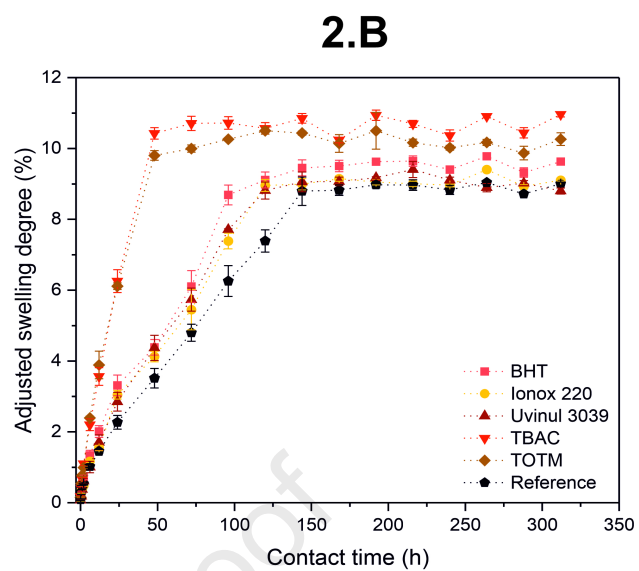
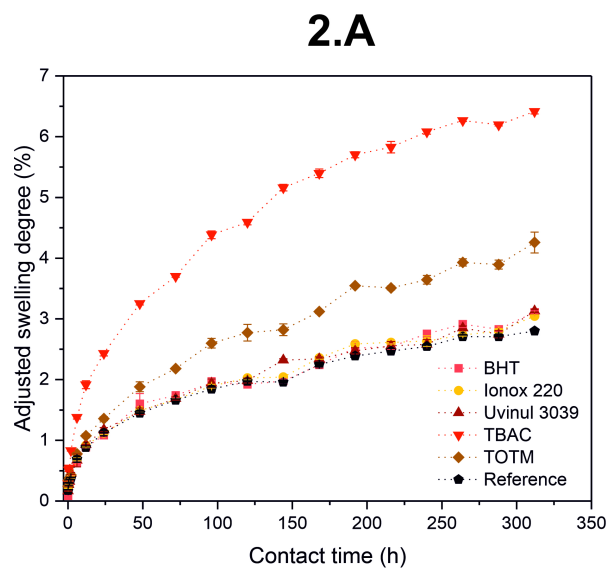
**All values are given as mean ± standard deviation.

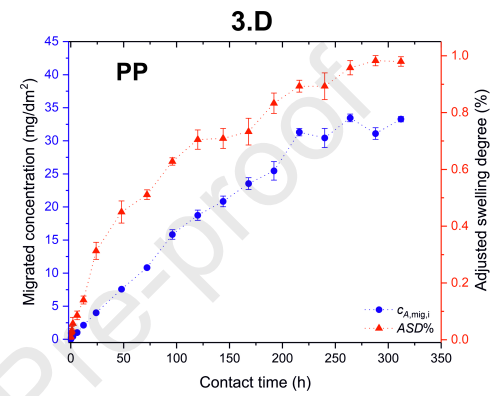
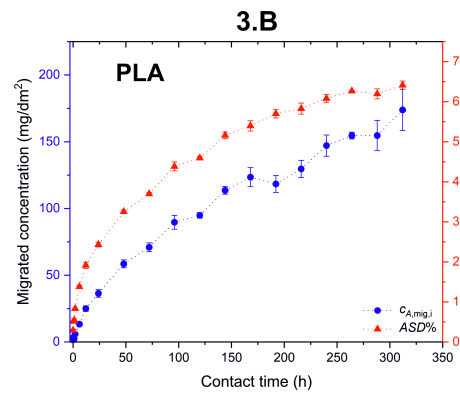
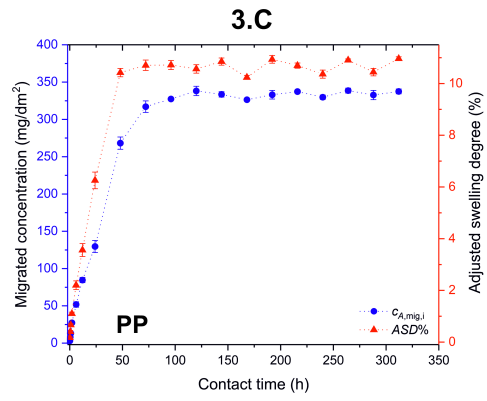
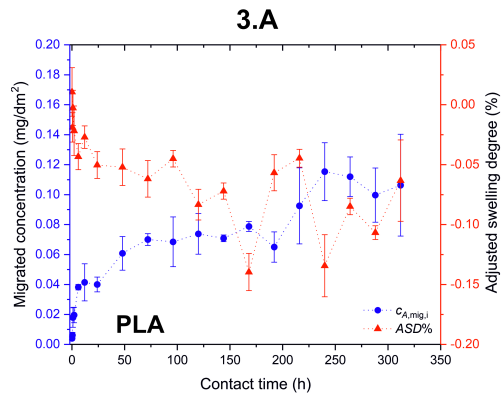
Table 3 Maximum surface normalized concentrations

<i>Additives</i>	<i>Maximum value of $c_{A,mig,i}$ (mg/dm²)</i>		
	<i>Isooctane</i>	<i>Ethanol 95 v/v%</i>	
PLA	BHT	0.0036 ± 0.0011	14.2 ± 1.06
	Ionox 220	0.0040 ± 0.0015	6.75 ± 0.972
	Uvinul 3039	0.0055 ± 0.00036	7.32 ± 0.514
	TBAC	0.11 ± 0.019	174 ± 15.3
	TOTM	0.043 ± 0.0082	34.1 ± 4.54
PP	BHT	48.2 ± 1.82	2.77 ± 0.138
	Ionox 220	31.1 ± 1.33	0.48 ± 0.040
	Irgafos 168	5.24 ± 0.150	0.032 ± 0.0010
	Uvinul 3039	32.2 ± 1.56	1.75 ± 0.067
	TBAC	339 ± 3.26	33.5 ± 0.581
	TOTM	327 ± 3.10	20.4 ± 0.776

*All values are given as mean ± standard deviation.

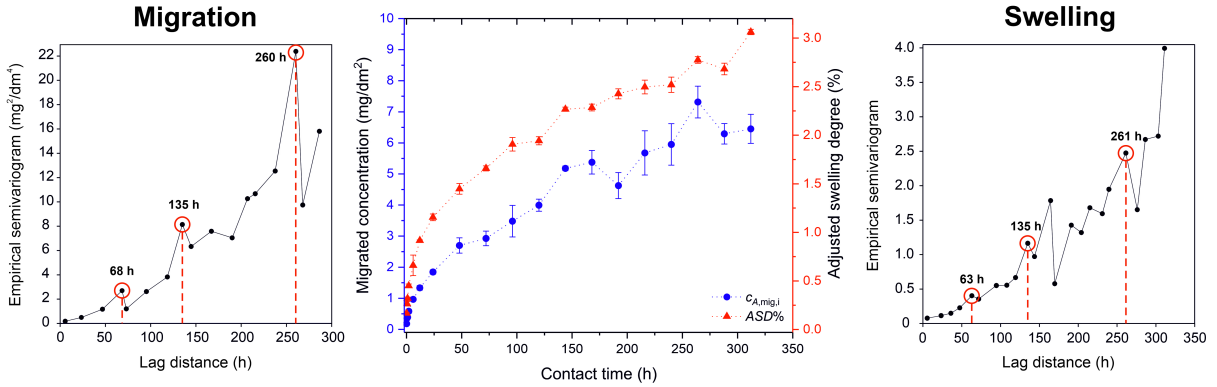






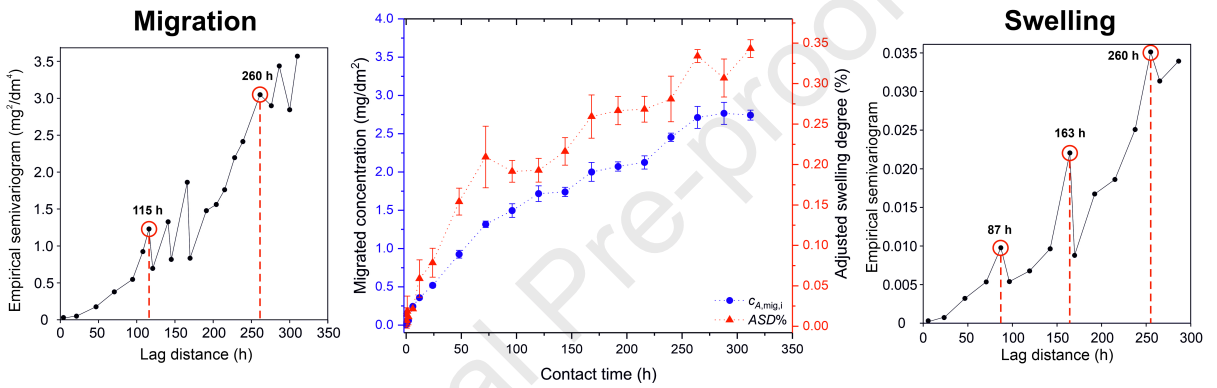
PLA – Uvinul 3039 – EtOH

5.A



PP – BHT – EtOH

5.B



Highlights

- Migration and swelling kinetics of polylactic acid and polypropylene were studied.
- Swelling strongly affects plastic additive migration from food contact materials.
- The effect of molecular weight on additive migration can be overruled by plasticizers.
- Variography was successfully applied to identify steady-states on kinetic curves.

Journal Pre-proof

Conflict of interest form

The authors:

Csaba Kirchkeszner^{a,b,‡}, Noémi Petrovics^{a,b, ‡}, Tamás Tábi^{c,d}, Norbert Magyar^e, József Kovács^f, Bálint Sámuel Szabó^{a,b}, Zoltán Nyiri^b, Zsuzsanna Eke^{a,g*}

^a Hevesy György PhD School of Chemistry, Eötvös Loránd University, Pázmány Péter stny. 1/A, H-1117 Budapest, Hungary

^b Joint Research and Training Laboratory on Separation Techniques, Institute of Chemistry, Eötvös Loránd University, Pázmány Péter stny. 1/A, H-1117 Budapest, Hungary

^c Department of Polymer Engineering, Faculty of Mechanical Engineering, Budapest University of Technology and Economics, Műegyetem rkp. 3, H-1111 Budapest, Hungary

^d MTA-BME Research Group for Composite Science and Technology, Műegyetem rkp. 3, H-1111 Budapest, Hungary

^e Department of Methodology for Business Analyses, Faculty of Commerce, Hospitality and Tourism, Budapest Business School, Alkotmány u. 9–11, H-1054 Budapest, Hungary

^f Department of Geology, Institute of Geography and Earth Sciences, Eötvös Loránd University, Pázmány Péter stny. 1/C, H-1117 Budapest, Hungary

^g Wessling International Research and Educational Center, Anonymus u. 6, H-1045 Budapest, Hungary

* Corresponding author.

‡ These two authors contributed equally to the work.

declare that they have no conflict of interest.